APL Photonics

10 GHz generation with ultra-low phase noise via the transfer oscillator technique

Cite as: APL Photonics **7**, 026105 (2022); https://doi.org/10.1063/5.0073843
Submitted: 04 October 2021 • Accepted: 24 January 2022 • Accepted Manuscript Online: 24 January 2022 • Published Online: 08 February 2022

N. V. Nardelli, T. M. Fortier, M. Pomponio, et al.

10 GHz generation with ultra-low phase noise via the transfer oscillator technique

Cite as: APL Photon. 7, 026105 (2022); doi: 10.1063/5.0073843
Submitted: 4 October 2021 • Accepted: 24 January 2022 •
Published Online: 8 February 2022

N. V. Nardelli,[1,2,a] T. M. Fortier,[1,a] M. Pomponio,[1,2] E. Baumann,[1,2] C. Nelson,[1] T. R. Schibli,[2] and A. Hati[1]

AFFILIATIONS

[1] National Institute of Standards and Technology, 325 Broadway, Boulder, Colorado 80305, USA
[2] University of Colorado, Boulder, Colorado 80309, USA

[a] **Authors to whom correspondence should be addressed:** nicholas.nardelli@nist.gov and tara.fortier@nist.gov

ABSTRACT

Coherent frequency division of high-stability optical sources permits the extraction of microwave signals with ultra-low phase noise, enabling their application to systems with stringent timing precision. To date, the highest performance systems have required tight phase stabilization of laboratory grade optical frequency combs to Fabry–Pérot optical reference cavities for faithful optical-to-microwave frequency division. This requirement limits the technology to highly controlled laboratory environments. Here, we employ a transfer oscillator technique, which employs digital and RF analog electronics to coherently suppress additive optical frequency comb noise. This relaxes the stabilization requirements and allows for the extraction of multiple independent microwave outputs from a single comb, while at the same time, permitting low-noise microwave generation from combs with higher noise profiles. Using this method, we transferred the phase stability of two high-finesse optical sources at 1157 and 1070 nm to two independent 10 GHz signals using a single frequency comb. We demonstrated absolute phase noise below −106 dBc/Hz at 1 Hz from the carrier with corresponding 1 s fractional frequency instability below 2×10^{-15}. Finally, the latter phase noise levels were attainable for comb linewidths broadened up to 2 MHz, demonstrating the potential for out-of-lab use with low SWaP lasers.

I. INTRODUCTION

High-stability microwave sources are ubiquitous in modern technology, underpinning communication, computing, and radar and sensing systems. Most of the latter systems rely on room-temperature crystal oscillators as local oscillators and frequency references. These commercially available electronic sources, however, exhibit phase noise that is unlikely to support next-generation systems that will require improved resolution and signal-to-noise ratios for higher density communications, micro-Doppler radar, and quantum sensing. More specifically, in Doppler radar, lower close-to-carrier phase noise would increase sensitivity to slow-moving objects or to objects with low cross sections.[1–3] This technique may also aid in the advancement of near-Earth asteroid mapping for both collision warning systems and for the detection of minerals for use on Earth or in space.[4] In wireless telecommunications, higher spectral purity would also permit lower error rates for phase-encoded signals and, thus, higher throughput.[5] Finally, sources with lower timing jitter could increase the resolution in analog-to-digital converters.[6]

Photonically generated microwave signals exploit the high quality-factors of ultra-stable optical references[7,8] to permit extraction of frequency-divided signals with ultra-low phase noise and high stability. To date, X-band signals near 10 GHz with the highest spectral purity have been achieved via optical frequency division (OFD) using self-referenced optical frequency combs (OFC).[3,9–13] Optical frequency combs based on mode-locked femtosecond lasers enable a phase-coherent link between the optical and microwave domains. When an OFC is phase stabilized to an ultra-narrow linewidth cavity-stabilized laser, designed to probe a long-lifetime atomic clock transition, it can permit extraction of a 10 GHz microwave signal with phase noise below −100 dBc/Hz at 1 Hz offset from carrier and with a signal-to-noise ratio close to 180 dB in a 1-Hz bandwidth.[11] Consequently, when

compared to other room-temperature oscillators, OFD allows for greater than 50 dB improvement in close-to-carrier phase noise sidebands.

Although OFD via phase-locked OFC (PL-OFD) has demonstrated record performance in the domain of room-temperature microwave generation, it suffers two drawbacks. First, it requires tight phase locking of the OFC to an optical reference. Depending on the feedback actuator bandwidth, tight phase locking may be insufficient in suppressing the additive noise of the OFC and may result in loss of phase lock. This is because the bandwidth of the actuator determines how quickly the feedback loop responds to changes in the laser frequency. Consequently, deviations in frequency with modulation frequencies outside the feedback loop bandwidth can result in loss of phase lock. Additionally, in the case of OFC noise that is high in relation to the actuator bandwidth, the comparators in the phase locked loops can result in poor determination of zero crossings, yielding cycle slips[14] that compromise the OFC microwave stability and timing. Similarly, cycle slips in the frequency counters can result in low stability in the measurement of the OFC-generated microwaves. Second, tight phase locking of an OFC generally only permits the derivation of low-noise microwave signals from a single optical reference. Consequently, each optical reference requires a corresponding OFC for division to the microwave regime, which may hinder technological implementation due to the increased power consumption and size.

The transfer oscillator (TO) technique[15] for OFD (TO-OFD) provides solutions to both of the aforementioned limitations. Rather than relying on physical actuators for phase-locking, the transfer oscillator technique employs electronics to add, subtract, and divide radio frequency (RF) signals in order to remove OFC phase noise from the divided-down optical reference. Due to the absence of physical actuators, the bandwidth of the TO electronics can be several megahertz, decoupling the optical-to-microwave division from the dynamics of the OFC and increasing the robustness of the generated microwave signals. Similar techniques have been used to characterize OFC offset frequency noise without an f-2f interferometer[16,17] and to generate low noise signals using a hybrid digital and optical setup to suppress noise.[18,19]

Notably, because OFD may be performed without phase-locking to an optical reference, the TO technique allows for the simultaneous generation of multiple microwave signals based on independent optical references. Since the OFC noise suppression is achieved in an external circuit, not in the OFC itself, a single OFC can perform optical-to-microwave division for multiple references. Consequently, absolute phase noise measurements between two or more divided-down optical references are possible using a single OFC.

These advantages help support the development of low-noise microwave flywheels derived from optical references, which are needed for realization of optical atomic time for future redefinition of the SI second.[20] Furthermore, TO-OFD may help to improve multi-frequency radar, which can provide high-resolution images for resource exploration and military ventures.[21] The TO technique may also help facilitate low-noise microwave generation from chip-scale OFCs that are difficult to stabilize[22] or from highly robust polarization-maintaining linear fiber lasers[23–26] that exhibit higher intrinsic noise.

In this work, we employ a free-space Er/Yb:glass optical frequency comb as a transfer oscillator to derive low phase noise 10 GHz microwave signals from optical reference cavities at 1157 and 1070 nm that serve as local oscillators for the Yb-lattice[27] and single-ion Al[28] clocks at NIST. Although the optical clocks were not operational for this work, the free-running optical references provided light with high-spectral purity and low drift ($\ll$1 Hz/s). From the latter optical references, we extracted two independent 10 GHz signals, using a single OFC, with absolute phase noise below −106 dBc/Hz at 1 Hz offset from carrier, and 1-s fractional frequency instabilities below 2×10^{-15}. To the best of our knowledge, the results we obtained represent the lowest close-to-carrier phase noise reported to date using the transfer oscillator technique, providing suppression of OFC noise in excess of 100 dB below a 1 Hz offset. It is also the first demonstration of the synthesis of multiple microwave signals based on independent reference cavities with a single OFC.

II. EXPERIMENTAL SETUP

Photonics-based microwave generation can be separated into three distinct experimental stages: (1) the optical reference that defines a lower limit to the system stability and phase noise, (2) the phase-coherent division performed by the optical frequency comb that enables faithful transfer of the optical reference stability and phase noise to the microwave domain, and (3) the electronic detection and synthesis, which includes photodetection as a means to demodulate the optical signals, and here, a digital transfer oscillator technique that enables electronic removal of OFC noise from the photodetected X-band microwave signals. In Sec. II, we describe the details of constituent components in our low-noise microwave generation setup and in Sec. III we describe their impact on the derived 10 GHz microwave signals.

A. Low-noise optical references

In this work, we employed optical references derived from lasers stabilized to state-of-the-art optical Fabry–Pérot cavities.[7,8] As mentioned previously, the optical reference sets the ultimate limit to the noise performance in photonic microwave generation via optical frequency division with an OFC. To minimize instabilities resulting from environmental effects, the cavities are housed within several layers of thermal and acoustic shielding and employ both passive and active vibration control to isolate the cavity length from changes due to acceleration. The room-temperature Fabry–Pérot cavities (~30 cm long) act as length references, which, at the time of the writing of this manuscript, can support fractional length instabilities near 1 part in 10^{16}. When a laser is stabilized to a longitudinal cavity mode, using high-bandwidth electro-optic phase modulators, the low phase noise and high fractional length stability of the cavity is transferred to the fractional frequency stability on the laser light. The latter can result in the realization of narrowed optical linewidths, near or below 100 mHz, on a 300 THz optical carrier. Currently, the uncertainty in the cavity length, for timescales greater than 1 s, is limited by thermally induced Brownian noise in the mirror coatings[29] and unidirectional length changes in the cavity due to settling of the ultra-low expansion glass that comprises the spacer. The low drift and thermal noise of the reference cavities can support phase noise as low as −120 dBc/Hz at a 1 Hz offset on a 10 GHz carrier.[2]

Shorter and smaller cavities, more suitable for portable optical atomic clocks and out-of-lab use, are also being actively developed.[30–32] Unfortunately, shorter cavity lengths naturally result in higher fractional length instabilities. The increased fractional instability, however, can be reduced by improving the cavity thermal noise. This can be achieved by using high-mechanical stiffness crystalline mirror coatings[32,33] that exhibit lower thermal noise and/or by using larger radius of curvature mirrors to increase the optical mode size for distribution of opto-mechanical pressure over a larger cross-section of the mirror substrate. The latter approach alone has yielded instabilities near 10^{-15} for cavity lengths of 25 cm[30] and instabilities of near 10^{-14} for cavity lengths of 5 cm.[31]

It has also been demonstrated that a free-running OFC can serve as its own optical reference cavity while simultaneously performing the optical-to-microwave division.[12] By employing a high-stability monolithic mode-locked laser, oscillator length fluctuations are minimized while simultaneously generating a coherent spectrum with which to link optical frequencies to microwave frequencies. While less complex, this solution only permits low phase noise at offset frequencies >10 kHz. Drift in the mode-locked laser cavity yields significantly higher noise than is possible when using Fabry–Pérot optical reference cavities.

B. Optical-to-microwave division: Er/Yb:glass OFC

Optical frequency combs, based on mode-locked laser spectra, permit phase coherent transfer of signals between the optical and microwave domains due to the fixed phase relationship between the resonant optical modes. As a result of this phase relationship, the optical spectra of OFCs consist of hundreds of thousands to millions of equidistant frequency modes where each individual mode of the OFC optical spectrum can be described by the following comb equation:

$$\nu_N = f_{\mathrm{ceo}} + N f_{\mathrm{rep}}, \tag{1}$$

where f_{ceo} (carrier-envelope offset frequency) is a frequency offset common to each optical mode, N is an integer representing the optical mode number, and f_{rep} (repetition frequency) is the optical mode spacing. We denote optical frequencies with the "ν" symbol and RF frequencies with the "f" symbol. Interference of the OFC light with single frequency light from an optical reference yields a heterodyne beat signal, $f_b = \nu_{\mathrm{opt}} - \nu_N$, between the optical frequency ν_{opt} and a nearby OFC mode ν_N.

By rewriting Eq. (1) as $(\nu_N - f_{\mathrm{ceo}})/N = f_{\mathrm{rep}}$, it is evident that frequency deviations on f_{rep} are N times smaller than those of the optical mode, ν_N. As a result, by referencing an OFC to a high-stability and low-noise optical reference, ν_{opt}, this frequency relationship between the optical and mode spacing of the OFC can be exploited to derive microwave signals with high spectral purity. Electronic signals derived in this manner also preserve the stability of the optical reference, such that, ideally $\sigma = \frac{\delta\nu}{\nu} = \frac{\delta f}{f}$. Additionally, photonically generated microwave signals permit a reduction in the phase noise of the optical reference by $(N/M)^2$ when photodetecting the Mth harmonic of the OFC repetition rate, f_{rep}. When dividing the 1157 nm (259 THz) and 1070 nm (280 THz) optical reference to 10 GHz, this results in a reduction in phase noise by 88.3 and 89.0 dB, respectively.

The optical frequency comb used in our measurements employs a home-built 1550 nm, 500 MHz repetition rate, free-space mode-locked laser based on Er/Yb co-doped phosphate glass.[34] Passive mode-locking, with an output power around 70 mW, is achieved in the laser via a semiconductor saturable absorption mirror (SESAM). The laser and its supporting optics are illustrated in Fig. 1.

The 500 MHz optical pulse train generated by the mode-locked laser is fiber-coupled and amplified in an Erbium doped fiber amplifier (EDFA) and then launched into a ~1 m highly nonlinear fiber (HNLF) to provide nonlinear frequency conversion from the input pulse at 1550 nm (bandwidth ~13 nm) to an optical octave of bandwidth (1–2 μm). The optical octave is coupled into free space, at which point a part of the spectrum is split off with a dichroic mirror and sent to a periodically poled lithium niobate (PPLN) waveguide to permit self-referenced detection of f_{ceo} via f-to-$2f$ conversion.[35,36] The remainder of the light is used to derive optical beat signals against the two high stability optical references at 1070 and 1157 nm.

The combined light from the OFC and optical references is sent through a two-stage pulse interleaver and focused onto a highly linear Modified Uni-Traveling Carrier (MUTC) photodetector (~12.5 GHz bandwidth, 50 μm active area diameter, −16 V bias).[37,38] The pulse interleaver effectively multiplies the pulse repetition rate from 500 MHz to 2 GHz,[10] increasing the strength of the recovered 10 GHz microwave tone, which consequently improves the thermally detected noise floor by mitigating photodetector nonlinearities that result at high optical pulse energies. Since the optical beat signals due to interference between the optical references and optical modes of the OFC are detected on the same MUTC photodiode, the RF output is split with a 1-to-4 power splitter, yielding four channels of similar microwave strength. The optical beats (f_{b1} and f_{b2}) and 10 GHz carrier (Mf_{rep}) are isolated from one another with narrow electrical bandpass filters. The beats of interest are displayed in bold red font in the RF spectrum of Fig. 1 lower-right inset.

Since TO-OFD permits the extraction of microwave signals via the removal of the additive OFC noise, the technique only requires control of the mode-locked laser oscillator length such that the optical beat does not drift outside a range bounded by $f_{\mathrm{rep}}/2$. In this experiment, the narrow-bandpass filters, mentioned above (bandwidth ≈5 MHz), are required to isolate the optical beats from nearby signals. To keep this beat centered on the narrow electronic filter, we employ a loose frequency lock (bandwith < 10 Hz) by monitoring f_{rep} and feeding back on the OFC cavity length. This maintains the optical beat close to the center of its bandpass filter. The f_{ceo} beat signal is uncontrolled as it drifts by only few MHz over the course of multiple days.

C. Microwave generation: Detection and transfer oscillator electronics

To generate a 10 GHz signal from the OFC, while simultaneously removing its noise contributions, the TO technique requires the detection of (1) the Mth harmonic of the OFC repetition frequency, Mf_{rep}, near 10 GHz, (2) the carrier-envelope offset frequency, $f_{\mathrm{ceo}} < 250$ MHz, and (3) the RF beat between each optical reference (subscript i) and the N_ith OFC mode, $f_{\mathrm{b,i}} = \nu_{\mathrm{opt,i}} - \nu_{N_i}$ also coincidentally near 10 GHz. The harmonic Mf_{rep} is chosen such that it is close to the desired output microwave carrier frequency

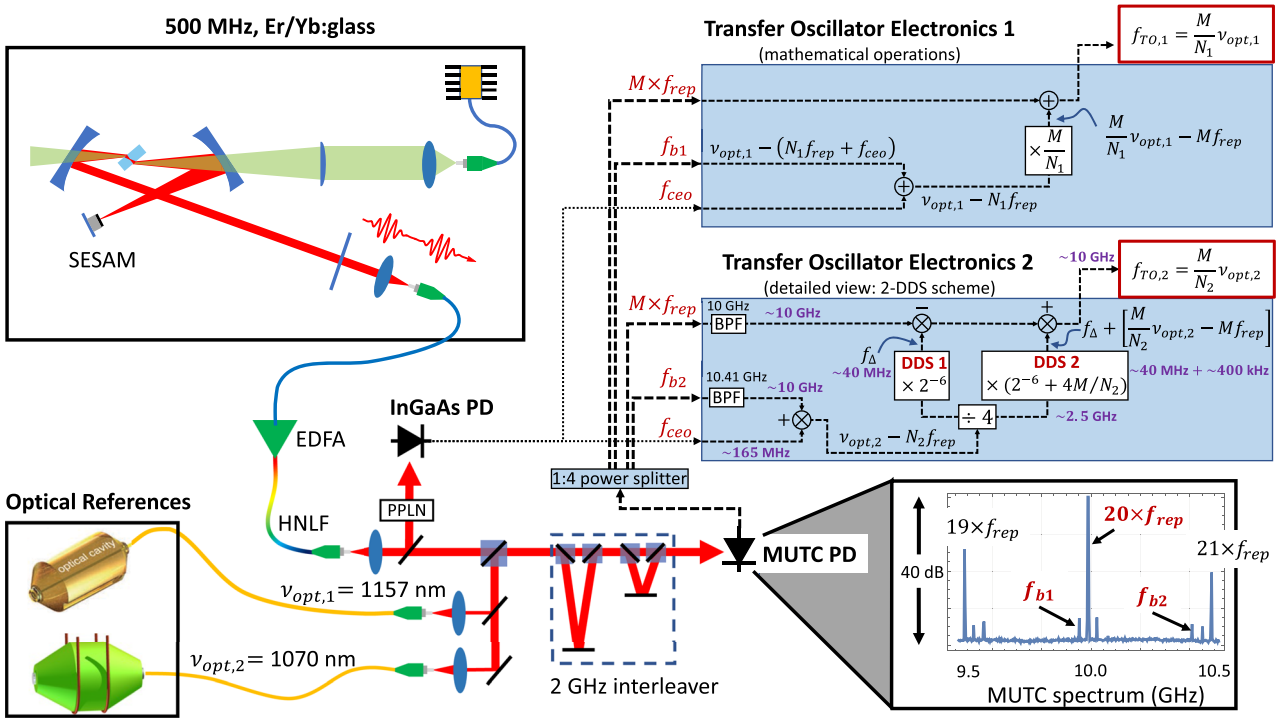

FIG. 1. Transfer oscillator setup with a 500 MHz repetition rate Er/Yb:glass OFC. Optical pulses from the Er/Yb:glass oscillator are fiber-coupled and amplified by an EDFA before being sent through an HNLF for supercontinuum generation. The spectrum is split in two paths, one for carrier-envelope offset frequency detection and the other for the detection of heterodyne beat signals between the OFC and light from two cavity-stabilized optical references at 1157 and 1070 nm. An optical interleaver multiplies the repetition frequency to 2 GHz, which is detected on an MUTC photodiode whose spectrum near 10 GHz is shown in the bottom-right inset (RBW = 300 kHz). The optical beats, f_{b1} and f_{b2}, and the M = 20 harmonic (bold red in the inset) of the 2 GHz pulses are sent to two TO circuits along with f_{ceo}. Each circuit generates a 10 GHz output, $f_{TO,i}$, that is derived from one of the two optical references by adding and dividing microwave signals, shown in blue boxes in upper right. Although the two TO electronics boards are identical, except for bandpass filters (BPF), to isolate f_{bi}, the top board in the figure is used to represent the transfer oscillator mathematical operations and the bottom board shows the 2-DDS scheme as well as the approximate RF frequencies at each stage. The following integer constants are used: M = 20, N_1 = 518 907, and N_2 = 561 211.

of 10 GHz. Here, $f_{b,i}$ was chosen to be near 10 GHz due to the availability of X-band electronics.

The three beat signals above are mixed such that

$$f_{TO,i} = Mf_{rep} + \frac{M}{N_i}(f_{b,i} + f_{ceo}) = \frac{M}{N_i}\nu_{opt,i}, \quad (2)$$

which yields a 10 GHz microwave signal free of OFC noise. The resultant microwave signal is dependent only on the static values of N_i and M and the optical reference frequency ν_{opt}. The electronics to facilitate the above signal processing are displayed pictorially in Fig. 1 and described in detail below.

(1) **Signal detection:** In our demonstration, we select the M = 20 harmonic of f_{rep} to generate a microwave carrier signal near 10 GHz. The high-power, high-linearity MUTC photodiode and the optical interleaver help to generate 1 dBm of microwave power at 10 GHz. The OFC mode numbers N_i with which the two optical references at 1157 and 1070 nm interfere are N_1 = 518 907 and N_2 = 561 211, respectively. From this, two optical heterodyne beat signals, $f_{b,1}$ and $f_{b,2}$, are derived near 10 GHz, with signal strengths varying from −80 to −65 dBm. A separate InGaAs photodetector (EOT 3000A) is used to detect f_{ceo}.

(2) **Removal of f_{ceo} noise:** Each detected heterodyne optical beat signal is routed to its own TO circuit and sent through a series of high-Q bandpass filters (bandwidth ≈5 MHz) to remove the high-power harmonics of f_{rep}. The filtered signal is then amplified to 10 dBm. The amplified beat is then used to drive the local oscillator (LO) port of an in-phase/quadrature (IQ) mixer (Marki MMIQ-0520L). The OFC offset frequency and its corresponding noise (f_{ceo} ≈ 165 MHz) are removed from $f_{b,i}$ using an IQ mixer and hybrid coupler with 30 dB of image rejection. This permits the addition or subtraction of signals without a band-pass filter to suppress the unwanted sideband. The result of this operation is $f_{b,i} + f_{ceo} = \nu_{opt,i} - N_i f_{rep}$, where $f_{b,i}$ has been expressed using Eq. (1). The removal of f_{ceo} has been previously demonstrated in photonic microwave generation[39] for the purpose of reducing the number of feedback loops.

(3) **Removal of optical noise on f_{rep}:** The goal of this step is to transform the $N_i f_{rep}$ on the right-hand side in the equation

in step 2 above to Mf_{rep} such that the outcome is $\frac{M}{N_i}[f_{b,i} + f_{ceo}] = \frac{M}{N_i}\nu_{opt,i} - Mf_{rep}$. With f_{ceo} removed, this latter signal is achieved by dividing the optical beat (≈10.165 GHz) by $N_1/M \sim 25\,900$ or $N_2/M \sim 28\,000$ to scale the optical OFC noise on the N_ith mode to Mf_{rep}. The f_{ceo}-free optical beat acts as the clock source for a Direct Digital Synthesizer (DDS, Analog Devices 9914), which divides the input by a factor of N_i/M, while also exhibiting low residual phase noise.[40] Because the maximum input clock frequency of the AD9914 is 3.5 GHz, we first digitally divided the 10.165 GHz amplified optical beat by 4. We adjusted, for this pre-division, by reducing the DDS division by a factor of 4.

To reach the final transfer oscillator output, $f_{TO,i} = \frac{M}{N_i}\nu_{opt,i}$, the additional Mf_{rep} must be removed from the right-hand-side such that $\frac{M}{N_i}[f_{b,i} + f_{ceo}] + Mf_{rep} = \frac{M}{N_i}\nu_{opt,i}$. The DDS-divided optical beat (near 400 kHz) is mixed with Mf_{rep} directly out of the photodiode, using an IQ mixer, to remove repetition rate noise contributed by the OFC. To drive the LO port of the mixer, the Mf_{rep} signal is amplified to 10 dBm with low phase noise amplifiers (Custom MMIC CMD245), which help preserve the ultra-low phase noise of the microwave carrier directly out of the OFC. This last step removes the multiplicative noise of f_{rep}, permitting the derivation of a microwave signal that only contains the frequency and phase noise of the optical reference. Additional optical references may be divided simultaneously with the OFC, each resulting in a corresponding microwave signal.

Phase noise spur suppression with two DDSs: The DDS output frequency $f_{DDS} = \frac{M}{N_i}[f_{b,i} + f_{ceo}]$ is close to 400 kHz, which, when mixed with Mf_{rep}, results in spurs that are harmonics of 400 kHz and that pose a challenge to filtering. To minimize these harmonics, two DDSs are employed to perform a dual heterodyne frequency translation:[41] DDS 1 synthesizes a frequency f_Δ, and DDS 2 synthesizes $f_\Delta + f_{DDS}$. Here, f_Δ is a frequency large enough to be filtered from the 10 GHz signal. We chose $f_\Delta \approx 40$ MHz, which corresponds to a division factor of 2^6, i.e., 2500 MHz/$2^6 \approx 40$ MHz.

The DDS 1 signal is subtracted from Mf_{rep} using an IQ mixer. The resulting signal $(Mf_{rep} - f_\Delta)$ is then added using a second IQ mixer to the DDS 2 signal. The result $(Mf_{rep} + f_{DDS})$ yields the same frequency as the 1-DDS scheme, but spurs due to mixing products are pushed to harmonics of $f_\Delta \approx 40$ MHz and its multiples that are more easily filtered from the 10 GHz tone. The 2-DDS scheme is shown pictorially in Fig. 1.

Imperfect spur suppression is mitigated by using a narrowband filter (bandwidth ≈5 MHz) between the aforementioned IQ mixers. While filtering reduces the 400 kHz phase noise spurs by nearly 40 dB, the filter introduces a significant group delay to the 10 GHz carrier signal. To ensure the highest bandwidth suppression of OFC noise, a delay line of several meters was added between DDS 2 and the second IQ mixer to compensate for the group delay of the filter.

III. RESULTS

In this section, we discuss characterization of the phase noise and stability of the 10 GHz output from our TO-OFD scheme.

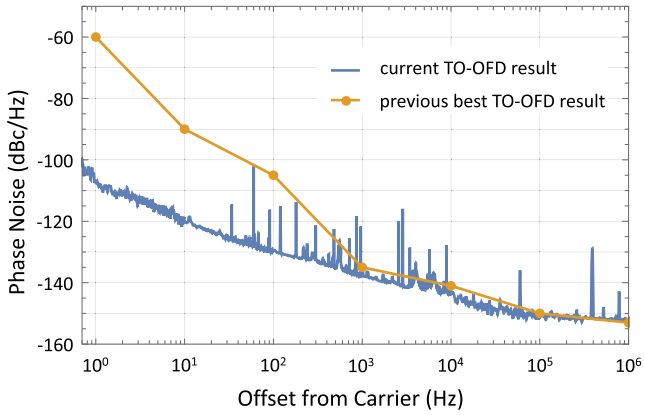

FIG. 2. Comparison between the current TO result (blue trace), the previous lowest phase noise TO result (connected orange dots).[41]

We specifically assess the difference in performance between OFD derived via TO-OFD and tight phase locking (PL-OFD) and characterize the limiting sources of noise in our TO scheme. Finally, we demonstrate noise suppression for optical linewidths as large as 2 MHz.

Figure 2 shows how the phase noise spectrum of the current demonstration compares to that of the previous best TO demonstration.[41] We show more than 40 dB of phase noise reduction at 1-Hz offset from carrier and a similar performance at high frequencies. This improvement was achieved by employing low phase noise optical references to be divided to microwave signals and low phase noise microwave references to adequately characterize the TO-generated signals. This improvement also necessitates the stringent accounting of noise sources, presented below, that were not significant enough in previous experiments to merit careful analysis.

A. 10 GHz characterization

The 10 GHz microwave signal generated by the transfer oscillator technique was compared against a reference 10 GHz signal derived from a Ti:sapphire OFC[2,42] [see Fig. 3(a)] that is phase-stabilized to the 1157 nm optical frequency reference. A 10 GHz tone, which was detected using an MUTC photodiode, was filtered and sent over ~3 m of microwave cable (Maury Microwave SB-SMAN-MM) to the Er/Yb:glass OFC and TO electronics. The frequency difference (≈1 MHz) between the two 10 GHz signals was measured using a Symmetricom 5125a digital phase noise analyzer. A 10 MHz H-maser signal served as the phase noise reference and contributed flicker phase noise near −120 dBc/f and a white phase noise floor near −160 dBc/Hz. We used this method to characterize the phase noise of each of the two $f_{TO,i}$ signals, derived from the 1157 and 1070 nm references, separately, and also the phase noise of Mf_{rep} generated via PL-OFD when the Er/Yb:glass OFC was phase-locked to one of the optical references.

As mentioned previously, TO-OFD allows for independent microwave signals to be derived from multiple optical references using a single OFC. We generated two distinct $f_{TO,i} \approx 10$ GHz microwave signals derived from the 1157 and 1070 nm cavity-stabilized lasers using two TO channels on the Er/Yb:glass OFC. The

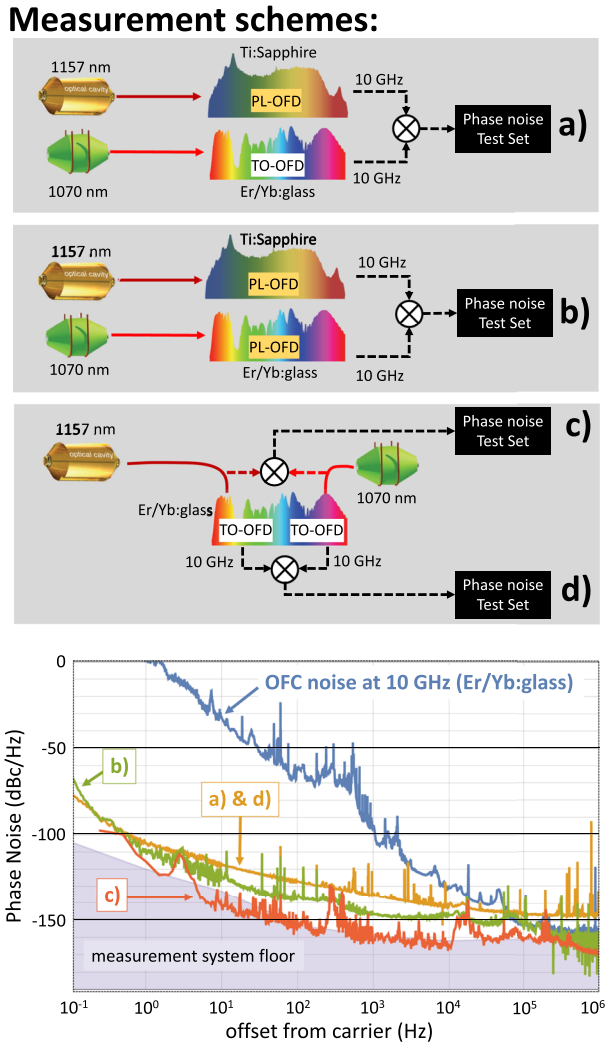

FIG. 3. Top: Microwave phase noise characterization setups for the measurements in the plot. Bottom: Phase noise comparison between Mf_{rep} generated by the Er/Yb:glass OFC when unstabilized (blue) and when stabilized to the 1070 nm optical reference (green) and $f_{TO,1}$ vs $f_{TO,2}$ when the OFC is unstabilized (orange). The 10 GHz limit (red) is set by the relative phase noise between 1157 and 1070 nm optical references, found by measuring the optical beat with an OFC and scaling to 10 GHz by subtracting 89 dB from the optical phase noise.

phase noise from this comparison is shown as the orange trace (d) in Fig. 3. A similar trace is seen when comparing the $f_{TO,i}$ signals against the 10 GHz produced with the locked Ti:sapphire [Fig. 3(a)]. Also seen in Fig. 3 is the free running noise on Mf_{rep} (blue trace). Using the TO technique, we observed suppression of unstabilized OFC noise of greater than 100 dB close to the 10 GHz carrier. Correspondingly, we observe fractional frequency instability suppression of the unstabilized carrier from more than 10^{-10} to less than 10^{-15} after 1 s of averaging.

The measurements in Fig. 3 all constitute absolute phase noise comparisons between microwaves generated from the 1157 and 1070 nm cavity-stabilized laser references. Microwaves produced via TO-OFD exhibited a 1 Hz phase noise level of ~−106 dBc/Hz, which we observed to be limited by the relative drift between the two optical references. This can be deduced from the relative optical phase noise of the 1157 and 1070 nm references, scaled to 10 GHz by a factor of $-20\log(280\ \text{THz}/10\ \text{GHz}) \approx -89$ dB. This measurement [Fig. 3(c)] represents the lower limit of 10 GHz phase noise that could be derived from these optical references.

Additionally, we compared the phase noise of the 10 GHz signal derived via PL-OFD when the Er/Yb:glass OFC was phase-stabilized to the 1070 nm optical reference against the 10 GHz signal generated via PL-OFD of the Ti:sapphire OFC, phase-stabilized to the 1157 nm optical reference. The resultant phase noise [Fig. 3(b)] demonstrates the contribution of the two OFCs and photodetection. From the comparison between green and orange traces, we observe that the 10 GHz electronic components in the TO technique (mixers, amplifiers, DDSs) limit the phase noise for frequency offsets 20 Hz and above.

B. Phase noise contributions

Here, we discuss the noise contributions to TO-OFD from its various components detailed in Sec. II. A summary of these contributions is enumerated and plotted in Fig. 4. Also shown is the quadrature sum of the individual noise sources (red trace), assuming that they are uncorrelated. Evident in Fig. 4, these sources account for most of the phase noise observed on the $f_{TO,i}$ signal (blue trace).

For offset frequencies less than 10 kHz, we observe that noise from the IQ mixers, which contribute flicker phase noise near −110 dBc/f, ultimately limits $f_{TO,i}$ phase noise. At high frequencies, the phase noise is limited by thermal noise, the dominant contributors of which are the two IQ mixers and three low phase noise amplifiers that combine the Mf_{rep} and the 40 MHz DDS outputs. The noise figures of the individual components, 10 dB for each mixer and 3 dB for each low phase noise amplifier, act in quadrature on the −7 dBm Mf_{rep} signal to yield a thermal limited noise floor of −153 dBc/Hz. We estimate that photodetector shot noise on Mf_{rep}, which takes into account photocurrent contributions from the single

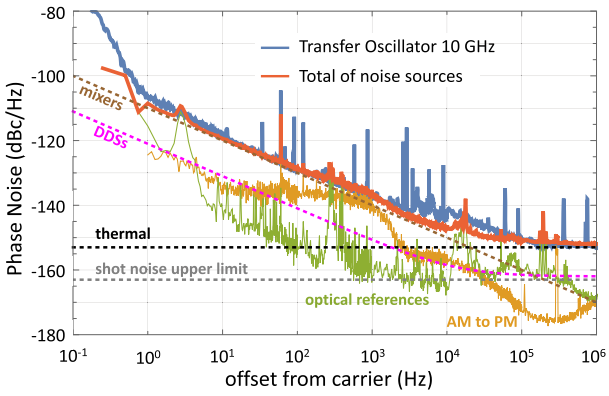

FIG. 4. Phase noise comparison between $f_{TO,2}$ derived from the 1070 nm reference (blue) and the total of all calculated noise sources (red). Constituent noise sources are plotted as dashed lines and thin traces.

frequency 1157 and 1070 nm light (1 mA) and the pulsed light from the OFC (7 mA), is less than −163 dBc/Hz.[43]

The DDS pairs employed in the TO circuits exhibit flicker (−121 dBc/f) and quantization noise (−162 dBc/Hz) on the $f_\Delta \approx 40$ MHz signal. One drawback of employing DDSs is that they contribute phase truncation spurs, with frequencies that depend on the division factor M/N_i and the frequency offset f_Δ. These spurs can be minimized by setting the DDS input/output ratio to be an exact multiple of 2, $f_{out} = 2^{-n} f_{in}$,[44] where n is a positive integer. It was not possible to implement this strategy in both DDSs because the DDS outputs are necessarily different. While not employed here, for applications that do not tolerate spurs, "bright" spurs can be traded for a slightly raised white noise floor by dithering the last bit in the DAC.[45] Finally, despite employing two DDSs to minimize the 400 kHz sidebands that result from $[f_{b,i} + f_{ceo}] \times M/N_i \approx 400$ kHz, imperfect mixing and filtering results in a residual spur at 400 kHz.

Additionally, quantization errors in the DDS can yield imperfect cancellation of OFC noise and drift in the derivation of the 10 GHz TO signal. To minimize rounding errors in the DDS, we have found that the choice of mode numbers is important to maximize the phase noise suppression of random frequency walk from the OFC. We estimate that a randomly chosen N/M could yield phase noise as large as −100 dBc/Hz at 1 Hz offset. Worse, using an incorrect value of N (i.e., N ± 1) can lead to a phase noise as high as −90 dBc/Hz at 1 Hz offset. These rounding issues can be circumvented altogether by using a DDS with a higher number of bits.

Due to the nonlinear elements in the TO setup (i.e., the photodiode, amplifiers, 10 GHz mixers), it is important to consider the effect of amplitude noise to phase noise conversion. To this end, we characterized the amplitude to phase noise conversion for our setup, including the contributions of the 10 GHz photodetector, TO electronic circuit, and 10 GHz phase noise comparison electronics. The characterization of the AM-to-PM (amplitude modulation-to-phase modulation) conversion coefficient is achieved by adding white amplitude noise to the laser by modulating one of the EDFA 980 nm pump diodes and measuring the RIN with a slow photodiode (Thorlabs PDA20CS). With the added RIN, we remeasured the $f_{TO,i}$ phase noise and discerned a single-sided AM-to-PM conversion of ~−32 dB. As seen via the orange trace in Fig. 4, using this conversion coefficient, we estimate the 10 GHz phase noise converted from RIN on the light incident on the MUTC photodetector (without added noise). Much of the RIN, we observed in this measurement, originated from the output of the semiconductor optical amplifier used to amplify the 1157 nm reference light. Amplification was not also required for the 1070 nm reference light since the OFC generated sufficient optical power at this wavelength to generate a high-SNR beat.

Finally, due to the relatively high flicker contribution from the IQ mixers, the combined phase noise of the optical references is only observed to impact the phase noise spectrum of $f_{TO,i}$ at low frequency offsets (less than 1 Hz). This noise is visible as a slope change in the absolute phase noise measurements that compare $f_{TO,1}$ and $f_{TO,2}$ derived from the 1157 and 1070 nm references. This thermal noise limit can be improved by operating the cavities at cryogenic temperatures or by employing high-quality factor mirrors with crystalline coatings.[33]

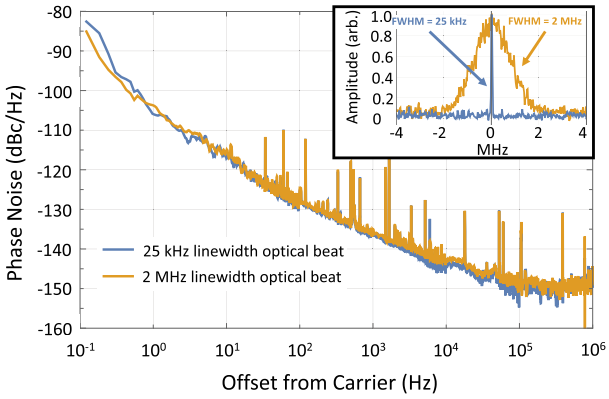

FIG. 5. Demonstration of noise suppression. Transfer oscillator microwave phase noise without added OFC frequency noise (blue) and with added OFC frequency noise (orange). Inset: the optical beat between a cavity stabilized laser and the comb, without and with added noise (blue and orange, respectively). Without added noise, the optical linewidth is 25 kHz, and with added noise, the optical linewidth is 2 MHz.

C. Frequency noise suppression

Due to the extremely high bandwidth of the digital and RF electronics, in principle, TO-OFD should permit near perfect cancellation of additive OFC noise for optical linewidths in excess of 1 MHz. As mentioned previously, noise suppression for microwave generation using the TO technique has direct application to field-deployable OFCs. In an attempt to quantify the cancellation, we increased the frequency noise on the OFC such that optical mode linewidths increased from 25 kHz to 2 MHz (near 1157 nm) by modulating an OFC laser mirror bonded to a fast PZT (PI Ceramic PL055.31) with white frequency noise. As seen in Fig. 5, we compare $f_{TO,i}$ with and without added frequency noise. We observe nearly identical phase noise spectra despite the difference in OFC optical linewidths. In this demonstration, the narrow-band bandpass filters used to isolate the optical beat signals limit the optical linewidth to around 2 MHz. Further added noise leads to a lower signal-to-noise ratio that results in high additive noise on the 2.5 GHz signals derived by the digital divide-by-4. Using a lower comb harmonic or a high-frequency DDS might permit a higher noise suppression bandwidth. Ideally, latency in the TO electronics, including the DDS, will set the noise suppression bandwidth. For the AD9914 DDS used here, the latency of a 2.5 GHz clock is ~150 ns, leading to a potential bandwidth greater than 1 MHz. This may be increased with a higher clock speed and a different choice of DDS.

Although TO-OFD demonstrates excellent frequency and phase noise suppression, it is unable to suppress noise resulting from AM-to-PM conversion. This may be dealt with by reducing the amplitude noise of the laser, for example, with active RIN suppression, or by operating the photodiode, amplifiers, and mixers under conditions where AM-to-PM conversion is naturally suppressed.[3,46,47]

D. Long-term behavior

While phase noise is used to evaluate the short term performance of the $f_{TO,i}$ microwave output (timescales less than

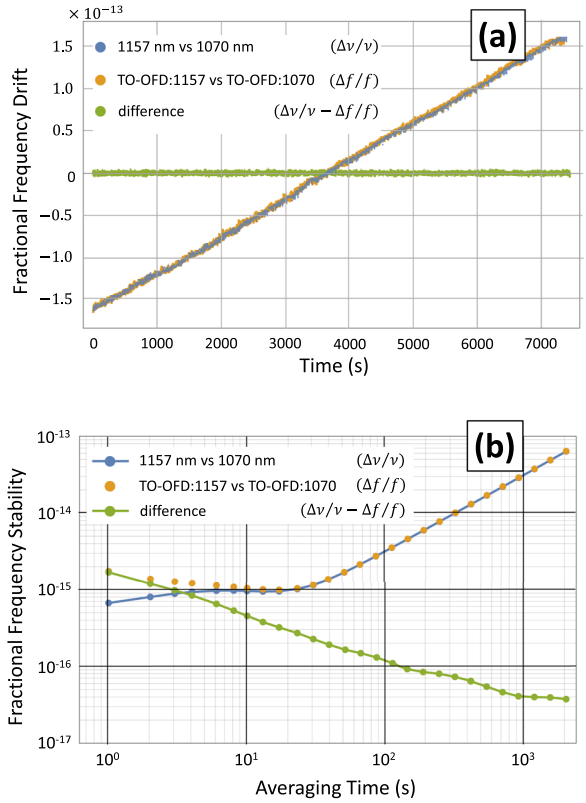

FIG. 6. (a) Time record and (b) Allan deviation of the optical beat between the 1157 and 1070 nm optical references (blue points) and the microwave beat (orange points) between $f_{TO,1}$ and $f_{TO,2}$ derived from the same optical references. The microwave beat is normalized by 10 GHz, and the optical beat is normalized by 280 THz in (a). The difference (green points) between the blue and orange points is shown in (a) and its Allan deviation is shown in (b).

1 s), we are also interested in assessing the long-term performance of the microwaves generated via TO-OFD (timescales up to 10 000 s). More specifically, we want to determine the fidelity with which the 10 GHz output reproduces the fractional frequency stability and variations of the optical references. To measure this, we simultaneously tracked the relative frequency drift of the 1157 and 1070 nm reference lasers in the optical domain using the Ti:sapphire OFC and the relative frequency drift between the two $f_{TO,i}$ signals produced using the Er/Yb:glass OFC from the same two optical references. Two Agilent 53131a frequency counters were used to collect data, each referenced to a 10 MHz H-maser signal.

As seen in Fig. 6(a), we observed a strong correlation between the time records of the fractional frequency deviations in the optical signals and microwave signals. The level of correlation is quantified by the residual deviations in the difference frequency. The Allan deviation evaluates the fractional frequency stability of this data as a function of measurement time. As seen in Fig. 6(b), the upper bound to the residual instability contributed by the Er/Yb:glass OFC and TO electronics is less than $2 \times 10^{-15}\tau^{-1/2}$.

IV. CONCLUSION

We have demonstrated microwave generation via optical frequency division of two high-stability optical references with absolute phase noise at or below −106 dBc/Hz at a 1 Hz offset from a 10 GHz carrier using the transfer oscillator technique. The latter result corresponds to a 1-s frequency instability of less than 2×10^{-15}, which indicates that the TO digital and analog electronics contribute minimal additional instability. This result represents the lowest-phase noise achieved, to date, using TO-OFD and is the first demonstration generating multiple independent optically derived microwave signals from a single OFC. In addition to characterizing and identifying the noise contributions to our transfer oscillator scheme, we have also demonstrated that the contribution of the OFC's noise to the TO signal is negligible for optical linewidths as large as 2 MHz, and OFC phase noise is suppressed by more than 100 dB close to carrier. This has direct application to low-noise microwave generation with more compact OFCs that exhibit high intrinsic noise. Additionally, TO-OFD provides the means to produce a reliable and robust optically derived microwave signal suitable for out-of-the lab applications.

Finally, the transfer oscillator technique provides significant advantages if used for realization of an optical timescale. Timescales derived from an ensemble of optical references permit a large reduction in frequency noise and a slower accumulation of timing uncertainty[48] than timescales based on microwave sources and references. The low residual noise and the increase of noise suppression bandwidth provided by TO-OFD will increase operational robustness and reduce the incidence of signal phase slips. Additionally, the ability to derive independent microwave signals from more than one optical reference may facilitate the redundancy necessary for deriving phase-continuous and high-stability electronic timing signals.

ACKNOWLEDGMENTS

We thank I. Coddington, S. A. Diddams, and F. Quinlan for their comments on this manuscript and J. C. Campbell for the MUTC photodiode.

Certain commercial equipment, instruments, or materials (or suppliers, or software, etc.) are identified in this paper to foster understanding. Such identification does not imply recommendation or endorsement by the National Institute of Standards and Technology, nor does it imply that the materials or equipment identified are necessarily the best available for the purpose.

AUTHOR DECLARATIONS

Conflict of Interest

The authors declare no conflicts of interest.

DATA AVAILABILITY

The data that support the findings of this study are available from the corresponding authors upon reasonable request.

REFERENCES

[1] J. Ye, J. L. Hall, and S. A. Diddams, "Precision phase control of an ultrawide-bandwidth femtosecond laser: A network of ultrastable frequency marks across the visible spectrum," Opt. Lett. **25**, 1675–1677 (2000).

[2]T. M. Fortier, M. S. Kirchner, F. Quinlan, J. Taylor, J. C. Bergquist, T. Rosenband, N. Lemke, A. Ludlow, Y. Jiang, C. W. Oates, and S. A. Diddams, "Generation of ultrastable microwaves via optical frequency division," Nat. Photonics **5**, 425–429 (2011).
[3]X. Xie, R. Bouchand, D. Nicolodi, M. Giunta, W. Hänsel, M. Lezius, A. Joshi, S. Datta, C. Alexandre, M. Lours, P.-A. Tremblin, G. Santarelli, R. Holzwarth, and Y. Le Coq, "Photonic microwave signals with zeptosecond-level absolute timing noise," Nat. Photonics **11**, 44–47 (2017).
[4]National Academies of Sciences, Engineering, and Medicine, *A Strategy for Active Remote Sensing Amid Increased Demand for Radio Spectrum* (National Academies Press, Washington, DC, 2015).
[5]S. Koenig, D. Lopez-Diaz, J. Antes, F. Boes, R. Henneberger, A. Leuther, A. Tessmann, R. Schmogrow, D. Hillerkuss, R. Palmer, T. Zwick, C. Koos, W. Freude, O. Ambacher, J. Leuthold, and I. Kallfass, "Wireless sub-THz communication system with high data rate," Nat. Photonics **7**, 977–981 (2013).
[6]G. C. Valley, "Photonic analog-to-digital converters," Opt. Express **15**, 1955–1982 (2007).
[7]M. Schioppo, R. C. Brown, W. F. McGrew, N. Hinkley, R. J. Fasano, K. Beloy, T. H. Yoon, G. Milani, D. Nicolodi, J. A. Sherman, N. B. Phillips, C. W. Oates, and A. D. Ludlow, "Ultrastable optical clock with two cold-atom ensembles," Nat. Photonics **11**, 48–52 (2016).
[8]B. C. Young, F. C. Cruz, W. M. Itano, and J. C. Bergquist, "Visible lasers with subhertz linewidths," Phys. Rev. Lett. **82**, 3799–3802 (1999).
[9]W. Zhang, Z. Xu, M. Lours, R. Boudot, Y. Kersalé, G. Santarelli, and Y. Le Coq, "Sub-100 attoseconds stability optics-to-microwave synchronization," Appl. Phys. Lett. **96**, 211105 (2010).
[10]A. Haboucha, W. Zhang, T. Li, M. Lours, A. N. Luiten, Y. Le Coq, and G. Santarelli, "Optical-fiber pulse rate multiplier for ultralow phase-noise signal generation," Opt. Lett. **36**, 3654–3656 (2011).
[11]T. M. Fortier, F. Quinlan, A. Hati, C. Nelson, J. A. Taylor, Y. Fu, J. Campbell, and S. A. Diddams, "Photonic microwave generation with high-power photodiodes," Opt. Lett. **38**, 1712–1714 (2013).
[12]M. Kalubovilage, M. Endo, and T. R. Schibli, "Ultra-low phase noise microwave generation with a free-running monolithic femtosecond laser," Opt. Express **28**, 25400–25409 (2020).
[13]T. Nakamura, J. Davila-Rodriguez, H. Leopardi, J. A. Sherman, T. M. Fortier, X. Xie, J. C. Campbell, W. F. McGrew, X. Zhang, Y. S. Hassan, D. Nicolodi, K. Beloy, A. D. Ludlow, S. A. Diddams, and F. Quinlan, "Coherent optical clock down-conversion for microwave frequencies with 10^{-18} instability," Science **368**, 889–892 (2020).
[14]L. C. Sinclair, J.-D. Deschênes, L. Sonderhouse, W. C. Swann, I. H. Khader, E. Baumann, N. R. Newbury, and I. Coddington, "A compact optically coherent fiber frequency comb," Rev. Sci. Instrum. **86**, 081301 (2015).
[15]H. R. Telle, B. Lipphardt, and J. Stenger, "Kerr-lens, mode-locked lasers as transfer oscillators for optical frequency measurements," Appl. Phys. B **74**, 1–6 (2002).
[16]A. Shehzad, P. Brochard, R. Matthey, F. Kapsalidis, M. Shahmohammadi, M. Beck, A. Hugi, P. Jouy, J. Faist, T. Südmeyer, and S. Schilt, "Frequency noise correlation between the offset frequency and the mode spacing in a mid-infrared quantum cascade laser frequency comb," Opt. Express **28**, 8200–8210 (2020).
[17]P. Brochard, S. Schilt, V. J. Wittwer, and T. Südmeyer, "Characterizing the carrier-envelope offset in an optical frequency comb without traditional f-to-$2f$ interferometry," Opt. Lett. **40**, 5522–5525 (2015).
[18]N. B. Hébert, A. P. Hilton, P. S. Light, and A. N. Luiten, "Hertz-level frequency comparisons between diverse color lasers without a frequency comb," Opt. Lett. **45**, 4196–4199 (2020).
[19]N. B. Hébert, S. K. Scholten, A. P. Hilton, R. F. Offer, C. Perrella, and A. N. Luiten, "Orthogonalizing the control of frequency combs for optical clockworks," Opt. Lett. **46**, 4972–4975 (2021).
[20]J. Yao, J. Sherman, T. Fortier, A. Ludlow, H. Leopardi, T. Parker, W. McGrew, S. Diddams, and J. Levine, "Optical-clock-based time scale," Phys. Rev. Appl. **12**, 044069 (2019).
[21]L. Pfitzenmaier, A. Battaglia, and P. Kollias, "The impact of the radar-sampling volume on multiwavelength spaceborne radar measurements using airborne radar observations," Remote Sens. **11**, 2263 (2019).
[22]E. Lucas, P. Brochard, R. Bouchand, S. Schilt, T. Südmeyer, and T. J. Kippenberg, "Ultralow-noise photonic microwave synthesis using a soliton microcomb-based transfer oscillator," Nat. Commun. **11**, 374 (2020).
[23]E. Baumann, F. R. Giorgetta, J. W. Nicholson, W. C. Swann, I. Coddington, and N. R. Newbury, "High-performance, vibration-immune, fiber-laser frequency comb," Opt. Lett. **34**, 638–640 (2009).
[24]L. C. Sinclair, I. Coddington, W. C. Swann, G. B. Rieker, A. Hati, K. Iwakuni, and N. R. Newbury, "Operation of an optically coherent frequency comb outside the metrology lab," Opt. Express **22**, 6996–7006 (2014).
[25]Y. Feng, X. Xu, X. Hu, Y. Liu, Y. Wang, W. Zhang, Z. Yang, L. Duan, W. Zhao, and Z. Cheng, "Environmental-adaptability analysis of an all polarization-maintaining fiber-based optical frequency comb," Opt. Express **23**, 17549–17559 (2015).
[26]A. Cingöz, D. C. Yost, T. K. Allison, A. Ruehl, M. E. Fermann, I. Hartl, and J. Ye, "Broadband phase noise suppression in a Yb-fiber frequency comb," Opt. Lett. **36**, 743–745 (2011).
[27]W. F. McGrew, X. Zhang, R. J. Fasano, S. A. Schäffer, K. Beloy, D. Nicolodi, R. C. Brown, N. Hinkley, G. Milani, M. Schioppo, T. H. Yoon, and A. D. Ludlow, "Atomic clock performance enabling geodesy below the centimetre level," Nature **564**, 87–90 (2018).
[28]S. M. Brewer, J.-S. Chen, A. M. Hankin, E. R. Clements, C. W. Chou, D. J. Wineland, D. B. Hume, and D. R. Leibrandt, "$^{27}Al^{+}$ quantum-logic clock with a systematic uncertainty below 10^{-18}," Phys. Rev. Lett. **123**, 033201 (2019).
[29]S. A. Webster, M. Oxborrow, S. Pugla, J. Millo, and P. Gill, "Thermal-noise-limited optical cavity," Phys. Rev. A **77**, 033847 (2008).
[30]J. Davila-Rodriguez, F. N. Baynes, A. D. Ludlow, T. M. Fortier, H. Leopardi, S. A. Diddams, and F. Quinlan, "Compact, thermal-noise-limited reference cavity for ultra-low-noise microwave generation," Opt. Lett. **42**, 1277–1280 (2017).
[31]M. L. Kelleher, T. Nakamura, J. Davila-Rodriguez, C. A. McLemore, J. P. Hendrie, S. A. Diddams, and F. Quinlan, "Centimeter-scale, rigidly held, thermal noise-limited optical cavity for mobile applications," in *Conference on Lasers and Electro-Optics* (Optical Society of America, 2021), p. STh4A.1.
[32]M. Giunta, J. Yu, M. Lessing, M. Fischer, M. Lezius, X. Xie, G. Santarelli, Y. Le Coq, and R. Holzwarth, "Compact and ultrastable photonic microwave oscillator," Opt. Lett. **45**, 1140–1143 (2020).
[33]G. D. Cole, W. Zhang, M. J. Martin, J. Ye, and M. Aspelmeyer, "Tenfold reduction of Brownian noise in high-reflectivity optical coatings," Nat. Photonics **7**, 644–650 (2013).
[34]D. M. B. Lesko, A. J. Lind, N. Hoghooghi, A. Kowligy, H. Timmers, P. Sekhar, B. Rudin, F. Emaury, G. B. Rieker, and S. A. Diddams, "Fully phase-stabilized 1 GHz turnkey frequency comb at 1.56 μm," OSA Continuum **3**, 2070–2077 (2020).
[35]H. R. Telle, G. Steinmeyer, A. E. Dunlop, J. Stenger, D. H. Sutter, and U. Keller, "Carrier-envelope offset phase control: A novel concept for absolute optical frequency measurement and ultrashort pulse generation," Appl. Phys. B **69**, 327–332 (1999).
[36]J. Reichert, R. Holzwarth, T. Udem, and T. W. Hänsch, "Measuring the frequency of light with mode-locked lasers," Opt. Commun. **172**, 59–68 (1999).
[37]Z. Li, Y. Fu, M. Piels, H. Pan, A. Beling, J. E. Bowers, and J. C. Campbell, "High-power high-linearity flip-chip bonded modified uni-traveling carrier photodiode," Opt. Express **19**, B385–B390 (2011).
[38]Z. Li, H. Pan, H. Chen, A. Beling, and J. C. Campbell, "High-saturation-current modified uni-traveling-carrier photodiode with cliff layer," IEEE J. Quantum Electron. **46**, 626–632 (2010).
[39]J. Millo, R. Boudot, M. Lours, P. Y. Bourgeois, A. N. Luiten, Y. L. Coq, Y. Kersalé, and G. Santarelli, "Ultra-low-noise microwave extraction from fiber-based optical frequency comb," Opt. Lett. **34**, 3707–3709 (2009).
[40]T. M. Fortier, A. Rolland, F. Quinlan, F. N. Baynes, A. J. Metcalf, A. Hati, A. D. Ludlow, N. Hinkley, M. Shimizu, T. Ishibashi, J. C. Campbell, and S. A. Diddams, "Optically referenced broadband electronic synthesizer with 15 digits of resolution," Laser Photonics Rev. **10**, 780–790 (2016).
[41]P. Brochard, S. Schilt, and T. Südmeyer, "Ultra-low noise microwave generation with a free-running optical frequency comb transfer oscillator," Opt. Lett. **43**, 4651–4654 (2018).
[42]T. M. Fortier, A. Bartels, and S. A. Diddams, "Octave-spanning Ti:Sapphire laser with a repetition rate >1 GHz for optical frequency measurements and comparisons," Opt. Lett. **31**, 1011–1013 (2006).

[43]F. Quinlan, T. M. Fortier, H. Jiang, A. Hati, C. Nelson, Y. Fu, J. C. Campbell, and S. A. Diddams, "Exploiting shot noise correlations in the photodetection of ultrashort optical pulse trains," Nat. Photonics **7**, 290–293 (2013).
[44]K. Gentile, "How to predict the frequency and magnitude of the primary phase truncation spur in the output spectrum of a direct digital synthesizer (DDS)," Application Note AN-1396, available online at https://www.analog.com/media/en/technical-documentation/application-notes/AN-1396.pdf.
[45]K. Gentile, "Section 11: Ancillary DDS techniques, features, and functions," available online at https://www.analog.com/media/en/training-seminars/design-handbooks/Technical-Tutorial-DDS/Section11.pdf, 1999.
[46]J. Taylor, S. Datta, A. Hati, C. Nelson, F. Quinlan, A. Joshi, and S. Diddams, "Characterization of power-to-phase conversion in high-speed p-i-n photodiodes," IEEE Photonics J. **3**, 140–151 (2011).
[47]F. N. Baynes, F. Quinlan, T. M. Fortier, Q. Zhou, A. Beling, J. C. Campbell, and S. A. Diddams, "Attosecond timing in optical-to-electrical conversion," Optica **2**, 141 (2015).
[48]W. R. Milner, J. M. Robinson, C. J. Kennedy, T. Bothwell, D. Kedar, D. G. Matei, T. Legero, U. Sterr, F. Riehle, H. Leopardi, T. M. Fortier, J. A. Sherman, J. Levine, J. Yao, J. Ye, and E. Oelker, "Demonstration of a timescale based on a stable optical carrier," Phys. Rev. Lett. **123**, 173201 (2019).